Original Contribution

A novel giant peroxisomal superoxide dismutase motif-containing protein

Diamandis Toutzaris [a,1], Jan Lewerenz [b,1], Philipp Albrecht [a], Laran T. Jensen [c], Julia Letz [b], Andreas Geerts [d], Stefan Golz [d], Axel Methner [a,*,1]

[a] Neurologische Klinik, Universitätsklinikum Düsseldorf, D-40225 Düsseldorf, Germany
[b] Neurologische Klinik, Universitätsklinikum Hamburg–Eppendorf, D-20246 Hamburg, Germany
[c] Johns Hopkins University, Baltimore, MD 21205, USA
[d] Institute for Target Research, Bayer HealthCare AG, 42096 Wuppertal/Germany

ARTICLE INFO

ABSTRACT

Oxidative glutamate toxicity in the neuronal cell line HT22 is a model for neuronal cell death by oxidative stress. In this model, extracellular glutamate blocks cystine uptake via the glutamate/cystine antiporter system x_c^-, eventually leading to depletion of the antioxidant glutathione and cell death. We used subtractive suppression hybridization and a screening procedure using various HT22 sublines to identify transcripts relevantly upregulated in resistance to oxidative glutamate toxicity. One of these coded for a novel protein of 3440 amino acids comprising a superoxide dismutase (SOD) motif, which we named TIGR for "transcript increased in glutamate resistance." TIGR is mainly expressed in the nervous system in cortical pyramidal and hippocampal neurons. Intracellularly, TIGR colocalizes with catalase, strongly suggesting a peroxisomal localization. Overexpression of TIGR but not of a mutant lacking two conserved histidine residues in the SOD motif increased SOD activity and protected against oxidative stress in mammalian cells, but had no direct SOD activity in yeast. We conclude that this novel giant peroxisomal protein is implicated in resistance to oxidative stress. Despite the presence of a SOD motif, which is necessary for protection in mammalian cells, the protein is not a functional SOD, but might be involved in SOD activity.

© 2010 Elsevier Inc. All rights reserved.

Neuronal cell death in diverse neurological disorders, including ischemic stroke and neurodegenerative diseases, can in part be attributed to excitotoxicity, in which excessive glutamate release overstimulates ionotropic glutamate receptors, resulting in massive calcium influx and cell death [1]. In addition to this rapid process, increased extracellular glutamate also leads to a more prolonged cell death by oxidative stress called oxidative glutamate toxicity. Here, the increased extracellular glutamate inhibits cystine import by blocking the gradient-driven glutamate/cystine antiporter system x_c^- [2,3]. Cysteine generated by intracellular reduction of cystine is required for the synthesis of glutathione (GSH), an important antioxidant in the brain [4,5]. GSH depletion renders the cells incapable of reducing reactive oxygen species, constantly produced in the mitochondria and during various enzymatic reactions, and ultimately causes cell death by oxidative stress. Oxidative stress is involved in the pathophysiology of Alzheimer's and Parkinson's disease, as well as ischemic stroke [6–9]. It was also recently shown in vitro that part of the cell death after excitotoxic stimuli can be attributed to oxidative glutamate toxicity [10].

Oxidative glutamate toxicity has been described in neuronal cell lines [2,11–14], immature primary neurons [3,12,15], oligodendroglia [16], and astrocytes [17]. The immortalized hippocampal cell line HT22 is an excellent model for studying oxidative glutamate toxicity, as it lacks ionotropic glutamate receptors [13] and responds to oxidative glutamate toxicity with programmed cell death in a very reproducible manner [18]. The sequence of events that leads to glutamate-induced cell death of HT22 cells involves depletion of intracellular GSH [12], activation of 12-lipoxygenase [19], accumulation of intracellular peroxides [20], and the activation of a cyclic GMP-dependent calcium channel close to the end of the death cascade [21].

We have used glutamate-resistant HT22 cells before to define the role of protective proteins such as the system x_c^- antiporter subunit xCT itself [22] or G-protein-coupled receptors [23,24] in resistance to oxidative stress. In this work, we used two paradigms to select HT22 cells resistant to glutamate and isolated clones upregulated in glutamate-resistant cells using subtractive suppression hybridization. These clones were then screened by reverse Northern blotting to identify transcripts matching the regulation patterns of known antioxidative transcripts such as the xCT subunit of the glutamate/cystine antiporter.

Materials and methods

Cell culture

Mouse HT22 cells were a gift from Professor Paschen, Max-Planck-Institute for Neurological Research (Cologne, Germany) and were

---

* Corresponding author. Fax: +49 21130203927.
  E-mail address: axel.methner@gmail.com (A. Methner).
[1] These authors contributed equally to this work.

cultured in DMEM (PAA Laboratories) supplemented with 5% FCS, 100 IU/ml penicillin, 100 µg/ml streptomycin, and 10 mM Hepes (pH 7.2). For selection of glutamate-resistant HT22 cells, 6×10^5 cells were seeded in 92-mm cell culture dishes (Nunc) and exposed to 10 mM glutamate after 24 h for 24 h. Surviving cells were expanded and again exposed to 20 mM glutamate under the same conditions, followed by two additional cycles of 20 mM glutamate with fewer cells (3×10^5) per dish. Then the cells remained exposed to 20 mM glutamate for 48 h during the last of the four selections. These cells were further cultivated in the presence of 10 mM glutamate and called chronic resistant HT22 cells (C+). Cells exposed to glutamate four times for 24 h that were further passaged in normal HT22 growth medium were called acutely glutamate-resistant HT22 cells (A). Neuro2a cells were obtained from DSMZ Braunschweig and cultured in high-glucose DMEM supplemented with 10% fetal calf serum, 100 IU/ml penicillin, and 100 µg/ml streptomycin. For stable transfections, cells were transfected with Lipofectamine 2000 (Invitrogen) and selected with 1000 µg/ml Geneticin (Invitrogen) for 3 weeks. Single colonies were isolated using cloning cylinders and transferred to 96-well plates for further expansion.

Viability assays

Cells (5×10^3) were seeded in 96-well plates and 24 h later exposed to glutamate or hydrogen peroxide (H_2O_2) for the time indicated. Viability was assayed 24 h later by the amount of blue formazan produced by viable cells from the tetrazolium salt 3-[4,5-dimethylthiazol-2-yl]-2,5-diphenyltetrazolium bromide (MTT; Sigma) as described [22,23].

mRNA isolation and cDNA synthesis

Wild-type (S), C+, and A cells (5×10^5 each) were seeded in 92-mm cell culture dishes in their appropriate medium and harvested either directly after 24 h of cultivation or (S and A cells only) after additional treatment with 10 mM glutamate for 6 h (designated S+ and A+, respectively). This treatment induced death in 50% of susceptible cells (data not shown). Total RNA was prepared using the TRIzol reagent (Life Technologies) and poly(A)$^+$ RNA enriched with the PolyATract mRNA isolation system (Promega). Double-stranded cDNA was generated from 2 µg poly(A)$^+$ RNA using the Universal Riboclone cDNA synthesis system (Promega) and the efficiency of first- and second-strand synthesis was monitored using [$\alpha-^{32}P$]dATP according to the manual.

Establishing cDNA libraries by suppression subtractive hybridization (SSH)

For SSH, *Rsa*I-digested adaptor-ligated cDNA libraries were constructed from double-stranded cDNA according to the PCR-Select cDNA subtraction kit (Clontech) manual. In summary, four subtracted libraries, S − C+, C+ − S, S+ − A+, and A+ − S+, were generated. PCR products from the secondary PCR of the subtracted library C+ − S were directly ligated into the plasmid vector pGEM-T Easy (Promega) and transformed into DH5α competent cells. Bacteria were plated on ampicillin-containing agar plates and incubated overnight, and clones with presumed cDNA inserts were identified by a white-blue screen using X-Gal and 0.1 M isopropyl-1-thio-β-D-galactoside.

Screening and sequencing of cDNA clones

Two hundred seventy white clones were randomly chosen and used to amplify the inserts by PCR with the np1 (5′-TCGAGCGG-CCGCCCGGGCAGGT-3′) and np2 (5′-AGCGTGGTCGCGGGCGAGGT-3′) primer pair included in the PCR-Select cDNA subtraction kit (Clontech) using 35 cycles; conditions were 94°C for 10 s, 68°C for 30 s, and elongation at 72°C for 90 s. Custom arrays of these clones were prepared in 10 copies by dotting 0.5 µl of each PCR product in duplicate on Porablot nylon membranes (Macherey–Nagel) using a 96-well dot-blot device (V&P Scientific). The arrays were hybridized with either radiolabeled (α-^{32}P) single-strand cDNA probes obtained by reverse transcription or random-labeled cDNA from subtracted libraries. Reverse-transcribed probes were synthesized in the presence of [α-^{32}P]dATP by Superscript reverse transcriptase (Invitrogen) of 0.5 µg poly(A)$^+$ mRNA. Single-stranded probes were generated from the forward and reverse subtracted libraries and PCR with primer np1 using the Strip-EZ PCR kit (Ambion) according to the manual. The specific activity of the cDNA probes was $>1 \times 10^9$ cpm/µg DNA. Equal amounts of heat-denatured ^{32}P-labeled cDNA probes ($\sim 2 \times 10^7$ cpm) from the subtracted libraries and from induced and uninduced cells were added to the hybridization solution (ExpressHyb; Clontech) and the membranes incubated at 68°C overnight. Nonspecific hybridization to the ubiquitous adaptor sequences was prevented by the addition of excess adaptor oligonucleotides. The membranes were washed under high stringency conditions and autoradiographed using a phosphoimaging system (Fujix) for various exposure times. Hybridization signal intensity was quantified using the VisualGrid software. Mean hybridization intensities above background of duplicate dots representing one fragment were calculated and normalized to Gapdh in the case of blots hybridized with cDNA. Dotted fragments that showed more than 2.5-fold higher hybridization signal using cDNA of one resistant HT22 cell strain and more than 3.0-fold upregulation using the other or more than 2.0-fold upregulation using both of the corresponding subtracted libraries in the absence of a contradictory result by hybridization with cDNA were further analyzed. The cDNA inserts of presumed differentially expressed clones were amplified under the above-described PCR conditions and sequenced by the dideoxy chain termination method using an Applied Biosystems automated DNA sequencer.

Northern blotting

Total RNA (5 µg) from S, S+, C+, A, and A+ cells grown under the same conditions as used for the generation of the subtracted libraries were separated by denaturing 1% agarose–formaldehyde gel electrophoresis and transferred to a nylon membrane. Radiolabeled probes were generated by linear PCR as described above using the adaptor-ligated fragments cloned from the subtracted library and either nested PCR 1 or primer 2 to obtain the strand complementary to the RNA. Probes specific for Gapdh, xCT, catalase, the γ-glutamylcysteine synthetase (γ-GCS) heavy chain, and GSH peroxidase were generated by random priming using the Megaprime DNA labeling system (Amersham Pharmacia Biotech). For the generation of the templates, fragments of the respective cDNAs were amplified from mouse brain cDNA using the following specific primers: 5′-ACCACAGTCCATGCCATCAC-3′ and 5′-TCCACCACCC-TGTTGCTGTA-3′ for Gapdh, 5′-TGTTCGCTGTCTCCAGGTTATTC-3′ and 5′-GCTTGCCTCACTGTATGACTT-3′ for xCT, 5′-AGAGGAAGGAGGCG-CATCA-3′ and 5′-CTGGGCCACTTTCATGTTCTCGT-3′ for the γ-GCS catalytic subunit, 5′-AGAAGCCTAAGAACGCAATTC-3′ and 5′-ATGT-GAAATCACTGCGTATTA-3′ for catalase, and 5′-GGCACCACGATCCGG-GACTA-3′ and 5′-TTAGGTGGAAAGCGATCGGGAAT-3′ for GSH peroxidase 1. PCR products were cloned into the vector pGEM-T Easy and sequenced. Northern blots were hybridized overnight at 42°C in ULTRAhyb solution (Ambion) with 10^6 cpm/ml radiolabeled probe, washed under high stringency conditions, and exposed to a phosphoimaging system (Phosphoimaging Device BAS2000; Fuji Photo Film GmbH) or Biomax MS films (Kodak) using an intensifying screen at −70°C for various exposure times. All blots were also hybridized with the probe for Gapdh. Autoradiographs obtained by phosphoimaging were further analyzed with the TINA 2.09 software (Raytest Isotopenmessgeräte GmbH) to calculate the photostimulated

luminescence above background and the ratio of regulation against Gapdh.

Cloning and overexpression of TIGR

Full-length TIGR was cloned by a combination of 5′-RACE (Clontech) from a fetal brain library purchased from Clontech and conventional cloning using ESTs. Full-length TIGR was sequenced by MWG Biotech using the primer walking technique and cloned into pENTR1a (Invitrogen) using EcoRI/NotI and into pcDNA3.1 HIS B (Invitrogen) using EcoRI/XbaI. To obtain an N-terminally enhanced green fluorescent protein (EGFP)-tagged TIGR construct, we moved the insert into pDEST-EGFP using the Gateway Cloning System (Invitrogen). Yeast expression plasmids for the TIGR clones were first generated by recombining into pYES-DEST52 (Invitrogen), resulting in galactose-inducible expression of the full-length TIGR sequence. Expression of the full-length TIGR clone in yeast resulted in toxicity, and plasmids expressing the putative superoxide dismutase 1 (SOD1) domain were generated by PCR amplification of the region corresponding to codons 1679 to 1831, introducing a start codon as part of a 5′ NdeI site and a stop codon followed by a 3′ SnaBI site. The PCR product was digested with the appropriate enzymes and ligated into pLS108 [25], replacing the ySOD1 coding sequence with that of the TIGR sequence, resulting in plasmid pLJ462.

Expression analysis by quantitative real-time PCR

For relative quantification of TIGR mRNA levels in human tissues, a TaqMan real-time PCR assay was used on a 7900 HT sequence detection system (Applied Biosystems) according to the manufacturer's protocols. For first-strand cDNA synthesis, 85 μg of total RNA was incubated for 1.5 h at 37°C with 2 units/μl Omniscript reverse transcriptase (Qiagen) in the supplied buffer plus 9.5 μM random hexamer primer, 0.5 mM each dNTP, and 3000 units of RNaseOUT (Invitrogen) in a final volume of 680 μl. The resulting cDNA was diluted 1:10 with water and directly used in PCR (5 μl per reaction). A PCR mix (20 μl) contained 0.2 μM each TIGR amplification primer (forward, 5′-AAGAAGATCTGTGGCGCAGT-3′; reverse, 5′-ACAGCTCT-CATCAGCAGCATA-3′), 0.2 μM FAM/TAMRA-labeled TIGR probe (5′-AGACTCCCTTCCACTCCCGTCAGC-3′), 0.2 mM each dNTP (including dUTP), 5 mM MgCl₂, uracil N-glycosylase, HotGoldStar DNA polymerase, and 5 μl template cDNA. The thermal protocol was set to 2 min at 50°C, followed by 10 min at 95°C and then 40 cycles of 15 s at 95°C and 1 min at 60°C. To normalize the amount of cDNA per assay, the expression of multiple housekeeping genes (e.g., hypoxanthine phosphoribosyltransferase, glyceraldehyde-3-phosphate dehydrogenase, and β-actin) was measured in parallel assays. The relative expression of TIGR was then calculated by using the normalized expression values.

Mouse mRNA abundance was quantitated using the qPCR core kit for Sybr Green I (Eurogentec) according to the manual. The mouse multiple-tissue cDNA panel (MTC; Clontech) served as template. PCR was done in triplicate with primers amplifying TIGR (5′-CCATGA-GATCCCGTTCCA-3′ and 5′-CCACAGTGGTTCGTTTGA-3′), β-actin (5′-AGGTCATCACTATTGGCAACGA-3′ and 5′-TTGGCATAGAGGTCTT-TACGGA-3′), and Gapdh (5′-AGGGTGGTGGACCTCATGGC-3′ and 5′-GGTGCAGCGAACTTTATTGAT-3′). Additionally, a standard dilution series of TIGR vector DNA was supplied as template to calculate amplification efficiencies, perform absolute quantification, and test for differences in efficiency between 96-well plates. All runs were analyzed using the SDS 2.1 software (Applied Biosystems). Baseline and threshold were optimized empirically, PCR efficiency was calculated using the slope of the regression curve fitted to the standard dilution C_T values. Relative regulation χ normalized to mean housekeeping gene regulation was calculated using the DCT method. Mean and standard error were calculated using Prism software (GraphPad).

Immunohistochemistry

We generated affinity-purified polyclonal antisera against two epitopes of TIGR. Rabbits were immunized against peptides corresponding to amino acids 1–16 and 3147–3162 coupled to KLH via a C-terminal cysteine (Eurogentec). Immunohistochemistry was performed on paraffin slices of brains of adult Wistar rats using a 1:50 dilution of the affinity-purified IgG antiserum and a biotinylated goat anti-rabbit IgG secondary antibody (1:200) and the biotin–streptavidin–HRP system Vectastain ABC-Elite (Vectorlabs) following the manufacturer's instructions. Before immunostaining, the slices were treated with 2.5 U/ml protease XXIV (Sigma) to demask the epitopes of interest.

Site-directed mutagenesis

To mutate the SOD motif in full-length TIGR, we first performed a PCR using pcDNA3.1 HIS B:TIGR as template using primers 5′-CTGCCACCTCTCTTCTTACACC-3′ and 5′-TCAGCTTGCAATTCCGAAC-CAG-3′. The PCR product was cloned into pGEM-Teasy (Promega) by TA cloning and histidine residues 1724 and 1726 were mutated to phenylalanine by site-directed mutagenesis using the QuikChange site-directed mutagenesis kit (Stratagene) according to the manual using the primers 5′-CACCGAGCTGCCCTCATTCTTAGCTCTTCTGG-3′ and 5′-CAGAAGAGCTAAGAATGAGGGCCGCTCGGTGC-3′. Finally, the mutated fragment was transferred back into the expression plasmid by using the restriction enzymes XbaI/SgrAI. The sequence integrity of these plasmids was ensured by double-stranded DNA sequencing (MWG Biotech and DNA Analysis Facility, Johns Hopkins University).

SOD activity

In Neuro2a cells, SOD activity was assessed by measuring the dismutation of superoxide radicals generated by xanthine oxidase and hypoxanthine using a superoxide dismutase assay kit (Cayman Chemicals) according to the manual. Yeast strains used to measure SOD activity were derived from EG103 (MAT α, leu2-3,112, his3Δ1, trp1-289, ura3-52) [26] and include KS107 (sod1Δ) [27] and LS101 (sod1Δ ccs1Δ) [25]. Yeast transformations were performed using the lithium acetate procedure as described [28]. Cells were propagated at 30°C either in enriched yeast extract, peptone-based medium supplemented with 2% glucose, or in synthetic complete medium. Solid medium was supplemented with 15 mg/L ergosterol and 0.5% Tween 80 to enhance growth under anaerobic conditions. Yeast strains lacking SOD1 activity display an oxygen-sensitive growth defect on medium lacking lysine [29], which can be used as an indirect assay for SOD1 activity. The copper chaperone CCS1 is needed for full activity of human SOD1. Yeast strains with the SOD1 or both the SOD1 and the CCS1 gene disrupted were transformed with the indicated plasmid and grown for 3 days on medium lacking lysine either in air or under anaerobic conditions using CO_2-enriched, oxygen-depleted culture jars (BBL GasPak; Becton–Dickinson).

Confocal microscopy

Neuro2a cells were seeded on coverslips and transfected 24 h later using Nucleofactor Kit R (Amaxa) with EGFP-TIGR. Cells were fixed for 20 min in 4% paraformaldehyde and stained with α-catalase (rabbit polyclonal; Epitomics; 1:100) and a secondary anti-rabbit antibody (Invitrogen) and visualized using a Zeiss LSM510 microscope.

Results

Generating HT22 cells resistant to oxidative glutamate toxicity

Exposing wild-type, glutamate-sensitive HT22 (S) cells for 24 h to 10 mM glutamate resulted in almost complete cell death. To obtain

glutamate-resistant cells, we exposed S cells to high concentrations of glutamate for 24 h. The few surviving cells were expanded and the procedure was repeated four times, which resulted in a new strain named HT22AR (A). We also generated a second strain named HT22CR (C) by extending the last cycle to 48 h and from then on propagating in the presence of 10 mM glutamate. These cells were described recently as HT22R cells [22,23]. The LD$_{50}$ of glutamate was increased ~25-fold in A and ~45-fold in C cells upon a 24-h treatment with glutamate. A cells tolerated up to 10 mM and C cells up to 20 mM glutamate without substantial reduction in viability (Fig. 1A).

Candidate protective transcripts are upregulated in resistant cells

Based on previous results from glutamate-resistant cells [22–24], we hypothesized that transcriptional changes might be involved in this resistance and focused on general transcriptional changes between C cells thriving in glutamate (C+), A cells with and without glutamate (A+ and A−), and S cells challenged with glutamate (S+). We hypothesized that those transcripts upregulated in C+ cells would encode proteins that confer the ability to constantly survive and proliferate under stress due to high extracellular glutamate. In contrast, A cells probably upregulate protective transcripts upon glutamate challenge, whereas S cells would regulate both apoptotic and protective transcripts.

We first investigated the expression of genes involved in glutamate toxicity and other known antioxidant genes to prove the assumed differences at the transcriptional level. We examined the mRNA expression of the enzyme γ-GCS and the transporter subunit xCT, as well as the classical antioxidant enzymes catalase and glutathione peroxidase 1 (GPx) by Northern blotting. The transporter subunit xCT was upregulated 7.1-fold in C+ cells and 3-fold in S+ cells, but less in A cells. The prototypic antioxidant catalase was upregulated 1.9-fold only in C+ cells, with no regulation in the other paradigms. γ-GCS was upregulated only 1.5-fold in C+ and even less in S+ and A+ cells. GPx was not regulated at all (Fig. 1B). Thus, C+ and A+ cells clearly differed in the expression patterns of these

protective transcripts, but did not show the expected concerted regulation. xCT and catalase were expressed in higher levels in the more resistant strain C+, whereas xCT and γ-GCS were upregulated in S cells during oxidative stress.

Suppression subtractive hybridization and screening identify other differentially regulated transcripts

From these experiments we concluded that C+ cells differ in the amount of neuroprotective transcripts. We still reasoned that transcripts upregulated not only in C+ cells, but simultaneously in A and in S cells challenged with glutamate, should be the most relevant and devised a complicated subtraction and screening procedure to identify these. We subtracted cDNA from S cells grown at a density that ensures susceptibility to glutamate-induced death from the cDNA of C+ cells grown at the same density in the presence of 10 mM glutamate and vice versa. The second subtracted pair consisted of S and A cells both exposed to 10 mM glutamate for 6 h, which led to approximately 50% cell death in S cells and no cell death in A cells (not shown). The inserts of 270 clones from the subtracted library C+ minus S were amplified by PCR, dotted onto eight identical blots, and hybridized with first-strand cDNA freshly generated from the original RNA samples or the subtracted libraries, respectively. The subtraction and hybridization strategy is depicted in Fig. 2A.

Six clones hybridized 2-fold better with the subtracted libraries C+ minus S and A+ minus S+ than with the reverse-subtracted libraries. Nine clones hybridized 2.5-fold better with cDNA from C+ and A+ compared to S. Clones with contradictory results between subtracted probes and cDNA were excluded. No clones hybridized with cDNA and the subtracted libraries. To exclude false positives, we hybridized these 15 clones to Northern blots to analyze their expression in C+ versus S cells and in A versus S with or without glutamate. All expression levels were normalized to Gapdh expression. Thirteen transcripts identified as positive in the screening procedure were not regulated more than 2-fold in C+ cells and were considered false positives. The remaining 2 clones were hybridized to two additional blots to calculate the mean ± SEM of regulation.

One clone corresponded to the dioxin-inducible cytosolic aldehyde dehydrogenase-3 (ALDH3), which labeled two transcripts of ~1.35 and ~3.2 kb in size. ALDH3 expression was prominently upregulated 3-fold in A and 2.1-fold in A+ cells compared to S cells under the same conditions. C+ cells showed a 1.7-fold upregulation. ALDH3 has already been implicated in response and protection against oxidative stress [30]. Another clone corresponded to a yet uncharacterized expressed sequence tag (EST; GenBank Accession No. aa94013) and labeled a very large message of approximately ~11 kb in the Northern blot. This transcript was upregulated ~3.1-fold in C+ and 1.6-fold in A+ cells compared to unchallenged S cells (Fig. 2B).

Cloning and characterization of the upregulated EST

We cloned EST aa94013 by a combination of bioinformatic analysis and 5′ RACE and named it TIGR for "transcript increased in glutamate resistance." Full-length TIGR matched the message of 11 kb seen on the Northern blot and contained an open reading frame of 3430 amino acids with a putative SOD motif according to Prosite (domain PS00087) in the central part of the protein. The sequence was submitted to GenBank with the submission ID GU433214. Whereas the mouse sequence contains one mismatch to this motif, the presumed human orthologue KIA0467 completely adheres to the consensus sequence. At the genomic level, TIGR consists of 87 exons and stretches over 61,158 bp on human chromosome 1p and 46,465 bp and 72 exons on mouse chromosome 4 (Fig. 3A). In mouse tissue, TIGR was expressed predominantly in brain and lung as shown by quantitative real-time PCR (Fig. 3B). We then immunized rabbits with peptides derived from the TIGR N- and C-termini and stained
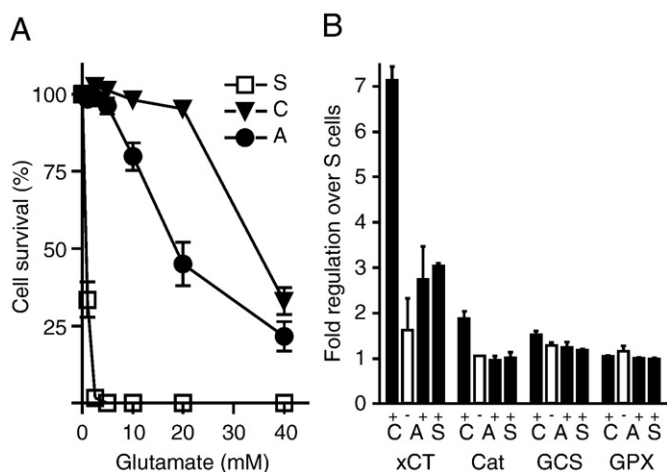

Fig. 1. Antioxidative transcripts are differentially regulated in cell lines resistant against oxidative stress. (A) Viability of wild-type (S) or two strains (A and C) of glutamate-resistant HT22 cells exposed to glutamate for 24 h. Relative survival was measured by the MTT assay normalized to cells not treated with glutamate. Each data point shows the mean ± SEM of three pooled independent experiments with n = 4. (B) Quantitative analyses of Northern blot experiments. Each blot contained 5 μg total RNA from the indicated cell lines with (+) and without (−) exposure to 10 mM glutamate for 6 h and was hybridized with radioactively labeled antisense probes against the mRNA of the antioxidant proteins xCT, catalase (Cat), γ-glutamylcysteine synthetase (GCS), and glutathione peroxidase (GPX). The housekeeping gene Gapdh was used as loading control. Bar graphs show the means ± SEM of regulation over Gapdh by comparing the band hybridization intensities from two duplicate blots.
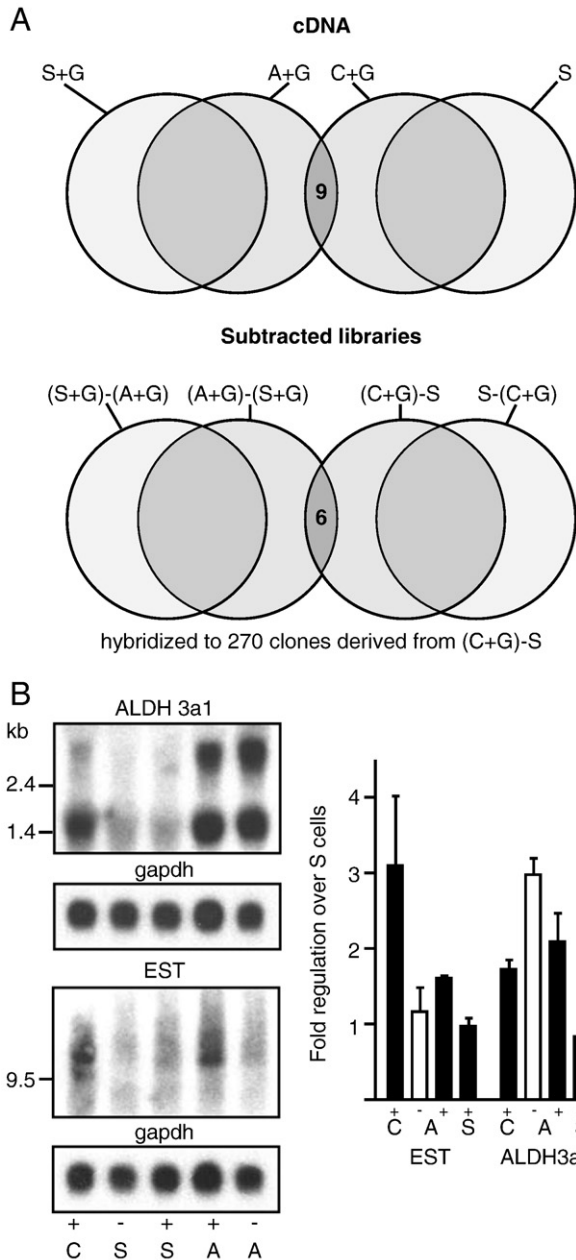
Fig. 2. RNA subtraction and screening by reverse Northern blotting identify an expressed sequence tag with an expression pattern resembling that of xCT. (A) 270 clones derived from the subtracted library C+ minus S were spotted onto eight identical blots (circles) and hybridized with the indicated cDNAs (top: 9 clones hybridized with A+ and C+, but not S+ and S) or subtracted libraries (bottom: 6 clones hybridized with A+ minus S+ and C+ minus S, but not S+ minus A+ and S minus C+). (B) Northern blot containing 5 μg total RNA from the indicated cell lines ± glutamate hybridized with antisense probes against ALDH3 or EST. The housekeeping gene Gapdh was used as loading control. The quantitative analysis shows the means ± SEM of regulation over Gapdh by comparing the band hybridization intensities from two blots.
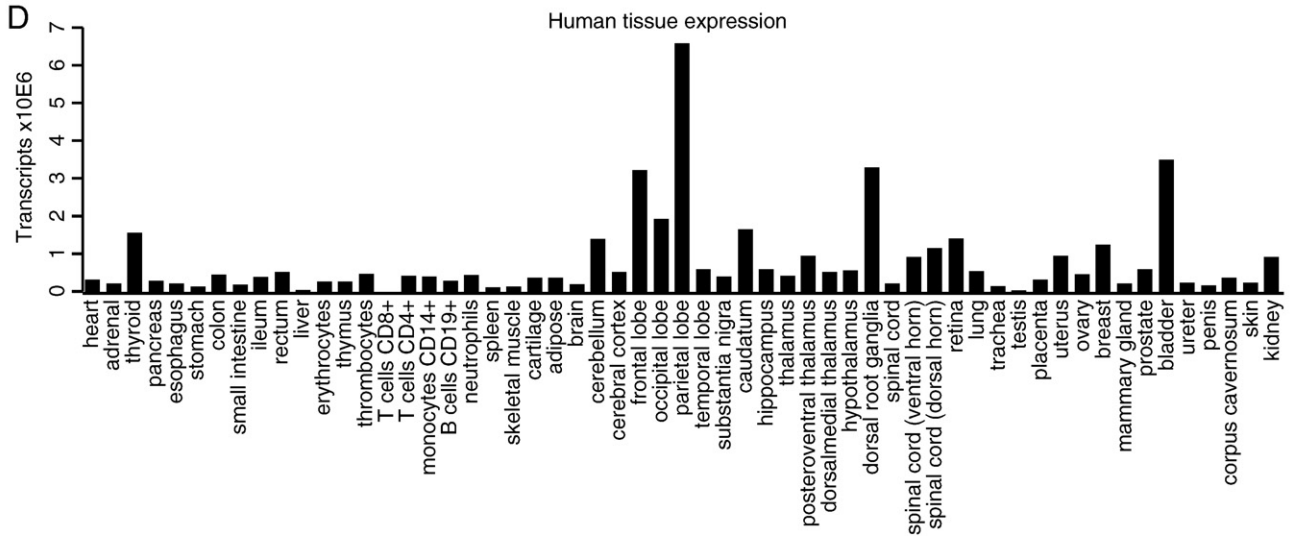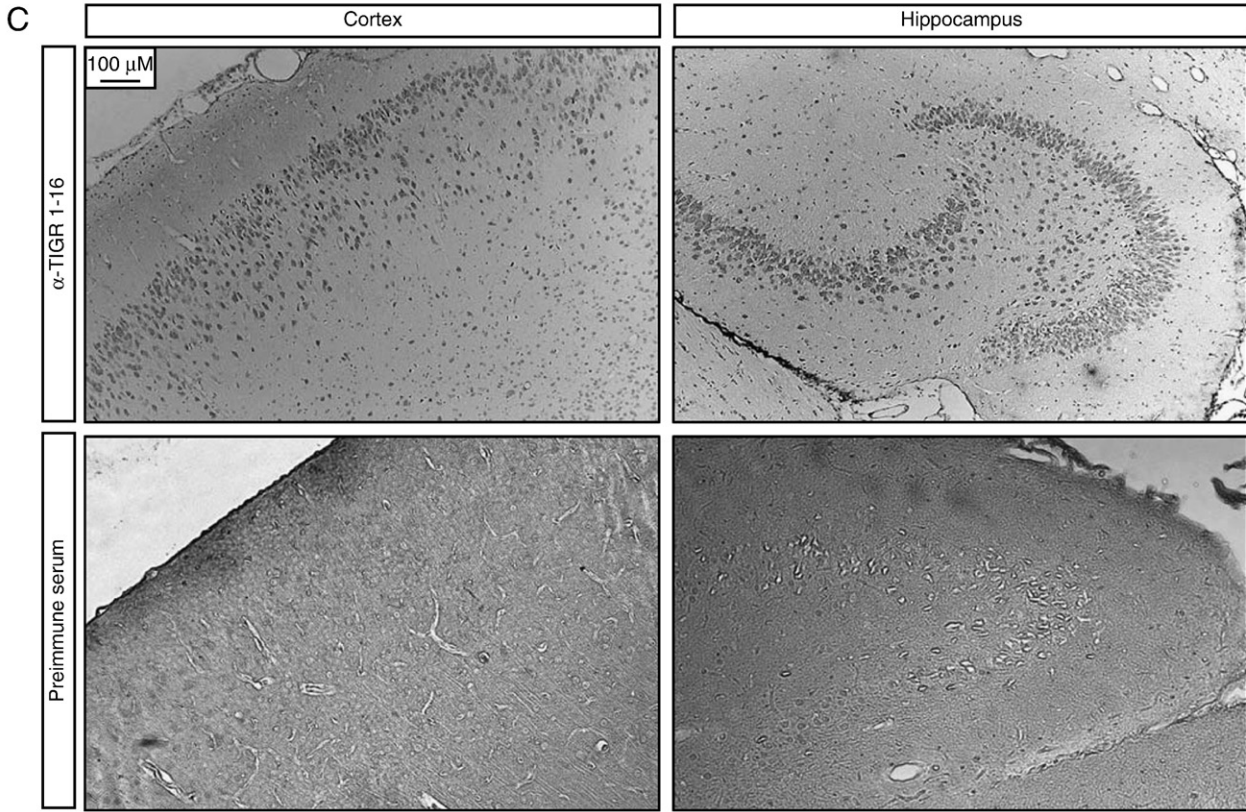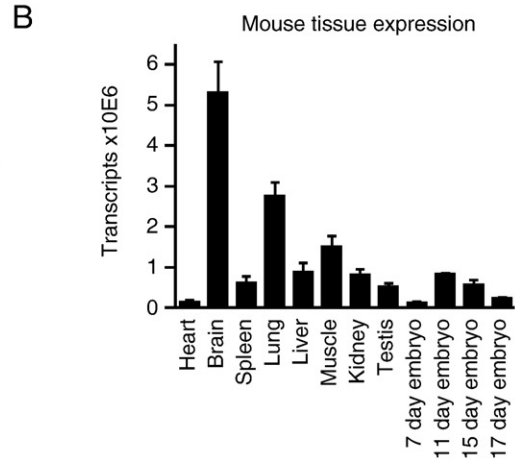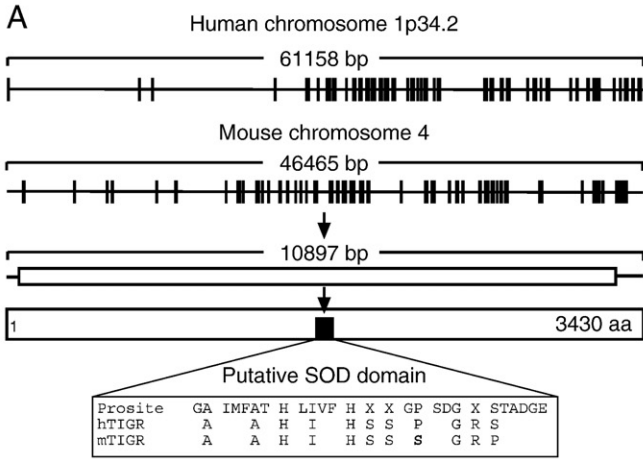
sections from rat brain with affinity-purified IgG antisera to investigate TIGR protein expression at the cellular level. Both antisera stained cells in the pyramidal layer of the rat cortex and hippocampal neurons, whereas the preimmune serum exhibited no specific staining pattern (Fig. 3C). Also in human tissues, TIGR was mainly expressed in the brain, predominantly in the parietal and frontal cortex as well as in dorsal root ganglia (Fig. 3D). We conclude that TIGR is a giant protein with a central SOD motif and a predominant neuronal expression pattern.

TIGR colocalizes with catalase in peroxisomes

Unfortunately, our antisera did not work in immunocytochemistry. We therefore fused TIGR N-terminally with EGFP to investigate its intracellular localization. Overexpressed EGFP-TIGR mainly localized in a particular perinuclear pattern reminiscent of peroxisomes (Fig. 4A). However, we also noted that a more cytosolic and less specific pattern prevailed when higher DNA concentrations of TIGR were transfected, which we interpreted as an artifact caused by massive overexpression (not shown). To prove the suspected peroxisomal localization, we overexpressed low amounts of EGFP-TIGR into HT22 S cells and stained with a monoclonal antibody against the peroxisomal marker protein catalase. Both proteins colocalized in immunofluorescence, proving the suspected peroxisomal localization of TIGR (Fig. 4B). To substantiate this on the genetic level, we searched for peroxisomal targeting signal 1 (PTS1), which is characteristic of many peroxisomal proteins. Indeed, the amino acids 497 to 508, SINQTDQMLAHL, matched the criteria for a PTS1 with a score of 5.058, which corresponds to 0.19 false positive hits [31]. We conclude that TIGR is a SOD-motif containing protein that colocalizes with catalase in peroxisomes when expressed in near physiological amounts. This is of utmost interest, as catalase metabolizes the product of SOD activity, H_2O_2, to water.

TIGR but not a mutant lacking two conserved histidine residues from the SOD motif protects against oxidative and ER stress

To investigate the suspected SOD activity in more detail, we cloned full-length TIGR into an expression vector and mutated two key histidine residues of the SOD motif [32] to alanines (HIH1724AIA) by site-directed mutagenesis. When transiently transfected into S cells, wild-type TIGR had no protective effect against oxidative glutamate toxicity, whereas mutant TIGR was clearly toxic (Fig. 5A). As a second cell stress agent we chose the N-glycosylation inhibitor tunicamycin, as C+ cells were previously shown to be similarly resistant against ER stress [23]. In this paradigm, we observed a weak protection conferred by wild-type, but not by mutated, TIGR (Fig. 5B). In these experiments, half of all transfected cells were treated with tunicamycin and the other half with glutamate. Transfection efficiency was monitored by cotransfection of EGFP. Therefore, we assume that changes in transfection efficiency cannot account for the observed differences in cell protection against oxidative and ER stress. To exclude an effect due to ectopic localization of strongly overexpressed TIGR, we also generated Neuro2a cells stably overexpressing wild-type and mutant TIGR. We chose Neuro2a cells because HT22 cells are resistant to most commonly used selection agents and therefore notoriously difficult to transfect stably. In these cells, both constructs were not excessively overexpressed and showed only a modest ~14- (wild type) or ~41-fold (mutant) upregulation compared to cells expressing lacZ as empty vector control, which were transfected and passaged in parallel with the TIGR cell lines. Therefore, mutant TIGR was approximately 3-fold more expressed than wild-type TIGR (Fig. 5C). Despite this, only wild-type and not mutant TIGR increased viability against 40 and 80 mM glutamate over control cells expressing lacZ (Fig. 5D). The high glutamate concentrations needed to kill these cells indicated that Neuro2a cells are relatively resistant to oxidative glutamate toxicity. Thus, we also used H_2O_2 as a second agent eliciting oxidative stress. At 750 μM, wild-type TIGR showed a significant advantage ($p < 0.05$; ANOVA) over the SOD mutant (Fig. 5E). There was no protection against tunicamycin, although we cannot exclude a protection against lower concentrations (Fig. 5F). We conclude that TIGR is upregulated in cells resistant to oxidative stress and that its overexpression protects against oxidative and ER stress. Although the protective effect seems to be rather modest it is clear that it depends on the integrity of the SOD motif, as mutated TIGR (in which only 2 of 3430 amino acids were changed by site-
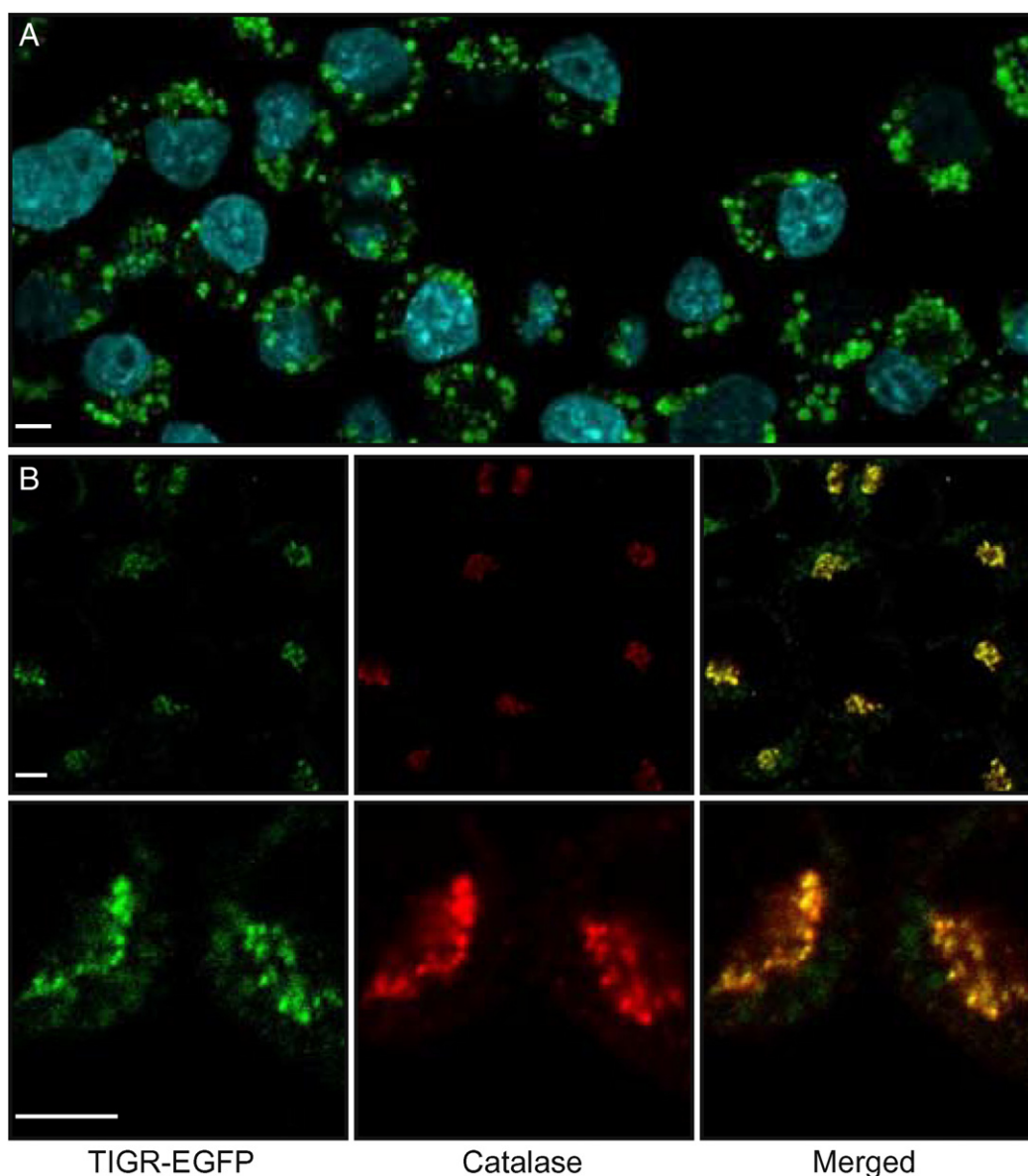
A Human chromosome 1p34.2
61158 bp

Mouse chromosome 4
46465 bp

10897 bp

1   3430 aa

Putative SOD domain

Prosite	GA	IMFAT	H	LIVF	H	X	X	GP	SDG	X	STADGE
hTIGR	A		A	H	I		H	S	S	P	G	R	S
mTIGR	A		A	H	I		H	S	S	*S*	G	R	P

B Mouse tissue expression

Heart, Brain, Spleen, Lung, Liver, Muscle, Kidney, Testis, 7 day embryo, 11 day embryo, 15 day embryo, 17 day embryo

C

	Cortex	Hippocampus
α-TIGR 1-16		
Preimmune serum		

100 μM

D Human tissue expression

heart, adrenal, thyroid, pancreas, esophagus, stomach, colon, small intestine, ileum, rectum, liver, erythrocytes, thymus, thrombocytes, T cells CD8+, T cells CD4+, monocytes CD14+, B cells CD19+, neutrophils, spleen, skeletal muscle, cartilage, adipose, brain, cerebellum, cerebral cortex, frontal lobe, occipital lobe, parietal lobe, temporal lobe, substantia nigra, caudatum, hippocampus, thalamus, posteroventral thalamus, dorsalmedial thalamus, hypothalamus, dorsal root ganglia, spinal cord, spinal cord (ventral horn), spinal cord (dorsal horn), retina, lung, trachea, testis, placenta, uterus, ovary, breast, mammary gland, prostate, bladder, ureter, penis, corpus cavernosum, skin, kidney

Fig. 4. TIGR colocalizes with catalase in peroxisomes. Confocal fluorescence microscopy of Neuro2a cells transiently overexpressing EGFP-TIGR and stained with (A) the nuclear marker DAPI or (B) α-catalase antibody as a peroxisomal marker. Scale bar, to 5 μm.

directed mutagenesis) had no protective effect at all despite a similar expression level and, when strongly overexpressed, even increased the sensitivity of HT22 S cells to oxidative glutamate toxicity.

TIGR increases SOD activity in Neuro2a cells but not in yeast

Based on the dramatic loss of function of the SOD point mutant lacking the two conserved histidine residues, we hypothesized that TIGR might be a novel giant SOD and investigated the SOD activity of the cell lines expressing wild-type or mutant TIGR using an enzymatic assay. SOD activity was assessed by measuring the dismutation of superoxide radicals generated by xanthine oxidase and hypoxanthine.

And indeed, only wild-type and not mutant TIGR significantly increased SOD activity in this assay (Fig. 6A).

We next studied this in a yeast system; however, expression of the full-length TIGR clone was toxic to yeast cells. Instead we expressed only the putative SOD domain and tested its ability to complement the oxygen-dependent lysine auxotrophy of sod1Δ yeast, which is a very sensitive assay for SOD activity. In this assay, human SOD1 fully restores growth in the absence of lysine in air (Fig. 6B), even in the absence of CCS1, which is required for full SOD1 activity [33]. However, neither the wild-type nor the mutant TIGR fragments were capable of restoring growth of yeast lacking SOD1 in the absence of lysine supplementation, suggesting that this region by itself may not contain SOD activity.

Fig. 3. The upregulated EST contains a SOD motif and is mainly expressed in the brain. (A) Bioinformatic analysis of TIGR showing chromosomal structure and localization of a conserved SOD motif according to Prosite. A mismatch in mouse TIGR is shown in bold. (B) Relative amounts of TIGR mRNA in mouse tissues measured by quantitative real-time PCR normalized to the expression of the housekeeping genes Gapdh and β-actin. (C) Immunohistochemistry using an antiserum generated against an N-terminal peptide of TIGR. Preimmune serum is shown as control. The magnification is indicated. (D) Relative amounts of TIGR mRNA in human tissues measured by quantitative real-time PCR normalized to the expression of the housekeeping genes hypoxanthine phosphoribosyltransferase, Gapdh, and β-actin.
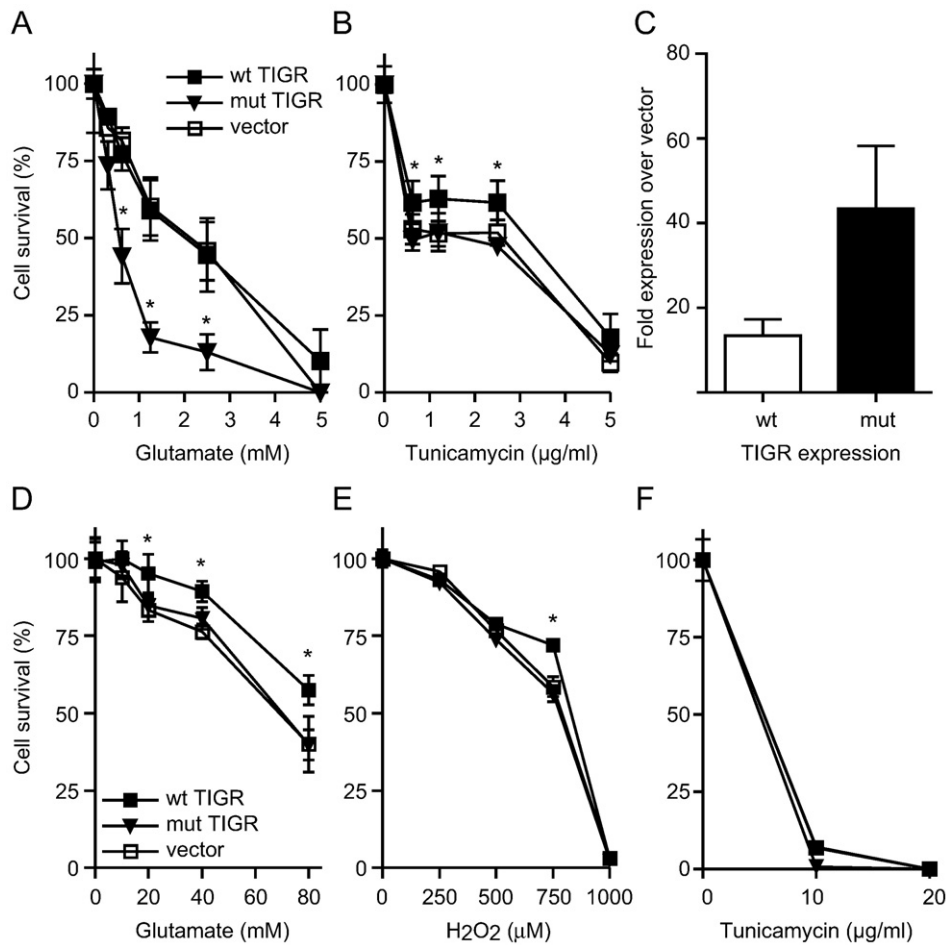
Fig. 5. TIGR protection against oxidative and ER stress correlates with its expression level. (A and B) HT22 S cells were transiently transfected with empty vector, wild-type TIGR (wt), or the HIH1724AIA mutant (mut TIGR) and exposed to the indicated concentrations of glutamate or tunicamycin for 24 h. (C) Neuro2a cells were stably transfected with the same constructs and expression of TIGR was measured by quantitative real-time PCR normalized to the expression of the housekeeping gene hypoxanthine phosphoribosyltransferase and shown as fold increase over TIGR expression in cells transfected with empty vector. (D–F) Stably expressing Neuro2a cells were exposed to the indicated concentrations of glutamate, H_2O_2, or tunicamycin for 24 h. Viability in (A and B) and (D–F) was quantitated by MTT assays. Relative survival was normalized to untreated cells. Each data point shows the mean ± SEM of three pooled independent experiments with $n = 4$; $*p < 0.05$, ANOVA with Dunnet's post hoc test.

Discussion

Treating HT22 cells repeatedly with toxic concentrations of glutamate followed by expansion of surviving cells led to the induction of a robust resistance to glutamate, which was further increased by constant cultivation in glutamate. This resistance was not specific to glutamate as at least the chronically resistant cell line C+ is similarly resistant to H_2O_2 [22], ER stress elicited by the
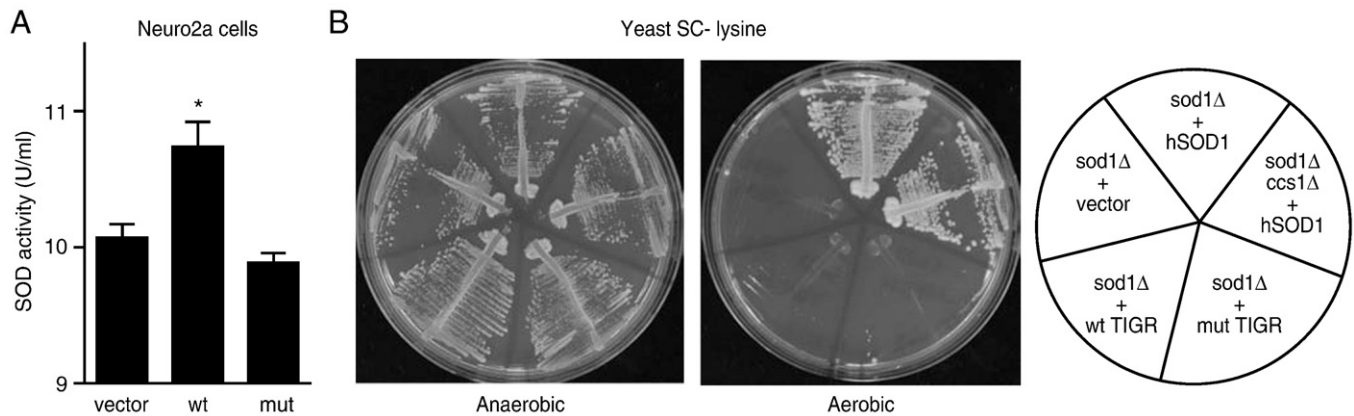

Fig. 6. TIGR increases SOD activity in Neuro2a cells but not in yeast. (A) SOD activity of Neuro2a cells stably overexpressing vector, TIGR (wt), or mutated TIGR (mut). SOD activity was assessed enzymatically by measuring the dismutation of superoxide radicals generated by xanthine oxidase and hypoxanthine. Bars show the means ± SEM of three pooled independent experiments with $n = 4$; $*p < 0.05$, ANOVA with Dunnet's post hoc test. (B) Yeast strains containing deletions in SOD1 (sod1Δ) or both SOD1 and CCS1 (sod1Δ ccs1Δ) were transformed with the indicated plasmid and tested for SOD activity using rescue of the oxygen-sensitive lysine defect as an assay. Yeast were grown either under anaerobic conditions as a control for toxicity of the TIGR clones or in air (aerobic).

N-glycosylation inhibitor tunicamycin, and overexpression of the proapoptotic protein Bax, a direct activator of the mitochondrial caspase cascade [23]. This is also in line with previous results [34] that showed glutamate-resistant cells to be resistant to cell death induced by Aβ, a pathogenic factor in Alzheimer disease. Thus, the mechanisms conferring resistance to glutamate could be of broader biological importance.

We examined the expression of four candidate antioxidant genes under five conditions to obtain a bar code for transcripts conferring glutamate resistance. However, only the xCT subunit of the cystine/glutamate antiporter showed a significant regulation in more than one paradigm and was upregulated in chronically resistant cells thriving in glutamate, as well as in acutely resistant and wild-type cells challenged with glutamate. The transcriptional upregulation of the xCT subunit in chronically resistant cells thriving in glutamate was previously shown by us [22] and is in line with the increased ability of similarly generated resistant HT22 cells to import cystine [34]. Catalase is one of the major H_2O_2-removing enzymes and its transcriptional upregulation is associated with an increased resistance to H_2O_2, emphasizing the functional relevance of this finding. Catalase activity was increased in glutamate-resistant HT22 cells generated separately from our cells, although catalase overexpression alone does not protect against oxidative glutamate toxicity [34]. γ-GCS is the rate-limiting enzyme in glutathione synthesis, and an increase in γ-GCS protein or activity was repeatedly found to be involved in protection against oxidative glutamate toxicity [35,36]. We could detect a very moderate upregulation of γ-GCS RNA in both resistant strains, similar to earlier reports, in which, however, only one of three resistant clones showed γ-GCS upregulation [34].

We next used a complicated subtraction and screening procedure to identify other transcripts of functional significance in this resistance. Only two clones showed regulation in more than one paradigm and none had exactly the same signature as xCT. The transcript of the dioxin-inducible ALDH3 was upregulated in both glutamate-resistant cell lines. Aldehyde dehydrogenases (aldehyde NAD(P)$^+$ oxidoreductase, EC 1.2.1.3) metabolize toxic aldehydes that accumulate during plasma membrane lipid peroxidation in response to oxidative stress [37]. ALDH3 is a cytosolic protein that is, depending on the tissue, either constitutively expressed or inducible [37]. It is part of the aromatic hydrocarbon-responsive gene battery and its regulation and role in oxidative stress were recently reviewed by Nebert [38]. Overexpression of human ALDH3 conferred resistance against induction of cell death by various medium-chain-length aldehydes and blocked the glutathione depletion induced by these [30]; aldehyde dehydrogenase activity in general was detected in neurons in the adult rat brain [39]. The upregulation of this transcript therefore proves the feasibility of our subtraction and screening approach.

The mRNA of the second upregulated transcript, which we named TIGR, was increased in C+ and in A cells challenged with glutamate. Its regulation pattern therefore closely resembles that of xCT, which was, however, also induced in wild-type cells treated with glutamate. TIGR is a completely uncharacterized gene; its human orthologue KIAA0467 was recently found to be potently induced by relA and a protein named transducer of regulated cAMP-response element-binding protein (TORC1), suggesting that its promoter has NF-κB and CRE-like sites [40]. Our immunofluorescence data and the identification of a PTS1 site in TIGR indicate that the new, giant 3430-amino-acid protein is part of the peroxisomal matrix. In addition to TIGR, another peroxisomal protein, catalase, was found to be upregulated by others [34] and by us (Fig. 1B) in cells resistant to oxidative glutamate toxicity. Proliferation of peroxisomes has been shown recently to be neuroprotective [41]. We conclude that TIGR might be involved in the neuroprotective function of peroxisomes.

TIGR contains a SOD motif (PS00082), which according to Prosite is found in only 174 of 470,369 proteins, 28 of which probably correspond to false positives. All false-positive proteins are of either bacterial or insect origin. The SOD motif is complete in human, dog, cow, and monkey, but contains a serine in mouse and rat and a lysine in chicken at position 8. However, TIGR does not contain a second Prosite SOD signature located in the C-terminal section of SOD proteins (PS00332). This motif is characterized by a cysteine involved in a disulfide bond and has a precision of 99.34% in detecting true and false positive hits, in contrast to 83.91% for motif PS00082. The fact that the potentially metal-binding histidines of TIGR are indispensable for its protection activity and that TIGR is found in peroxisomes in close proximity to catalase, which catalyzes the removal of H_2O_2, the product of SOD, suggest a function as SOD. However, this was not the case in a yeast assay for SOD activity. There are, however, certain caveats with this assay. First, we could not use full-length TIGR in this assay, as it was toxic to the cells. Second, it is possible that cofactors needed for the SOD-like function of TIGR might not be present in yeast. It is certainly possible that TIGR itself has no SOD activity but assists other proteins by stabilizing the metal cofactors copper and zinc in the active core of real SOD enzymes. The conflicting results with regard to cell protection observed by us might be explained by differences between transient and stable transfection on the expression level of TIGR, as we observed that strong overexpression of TIGR—as is easily achieved by transient transfection—altered its intracellular localization. On the other hand, long-term stable over-expression might lead to compensatory changes and subsequent upregulation of additional cofactors needed for optimal protection by TIGR. It is evident that more has to be done at the protein level, which, considering the sheer size of this protein, is beyond the scope of this contribution.

References

[1] Choi, D. W. Glutamate neurotoxicity and diseases of the nervous system. Neuron 1:623–634; 1988.
[2] Murphy, T. H.; Miyamoto, M.; Sastre, A.; Schnaar, R. L.; Coyle, J. T. Glutamate toxicity in a neuronal cell line involves inhibition of cystine transport leading to oxidative stress. Neuron 2:1547–1558; 1989.
[3] Murphy, T. H.; Schnaar, R. L.; Coyle, J. T. Immature cortical neurons are uniquely sensitive to glutamate toxicity by inhibition of cystine uptake. FASEB J. 4:1624–1633; 1990.
[4] Schulz, J. B.; Lindenau, J.; Seyfried, J.; Dichgans, J. Glutathione, oxidative stress and neurodegeneration. Eur. J. Biochem. 267:4904–4911; 2000.
[5] Dringen, R.; Gutterer, J. M.; Hirrlinger, J. Glutathione metabolism in brain metabolic interaction between astrocytes and neurons in the defense against reactive oxygen species. Eur. J. Biochem. 267:4912–4916; 2000.
[6] Beal, M. F. Mitochondria, free radicals, and neurodegeneration. Curr. Opin. Neurobiol. 6:661–666; 1996.
[7] Coyle, J. T.; Puttfarcken, P. Oxidative stress, glutamate, and neurodegenerative disorders. Science 262:689–695; 1993.
[8] Pratico, D. Alzheimer's disease and oxygen radicals: new insights. Biochem. Pharmacol. 63:563–567; 2002.
[9] Halliwell, B. Reactive oxygen species and the central nervous system. J. Neurochem. 59:1609–1623; 1992.
[10] Schubert, D.; Piasecki, D. Oxidative glutamate toxicity can be a component of the excitotoxicity cascade. J. Neurosci. 21:7455–7462; 2001.
[11] Miyamoto, M.; Murphy, T. H.; Schnaar, R. L.; Coyle, J. T. Antioxidants protect against glutamate-induced cytotoxicity in a neuronal cell line. J. Pharmacol. Exp. Ther. 250:1132–1140; 1989.
[12] Davis, J. B.; Maher, P. Protein kinase C activation inhibits glutamate-induced cytotoxicity in a neuronal cell line. Brain Res. 652:169–173; 1994.
[13] Maher, P.; Davis, J. B. The role of monoamine metabolism in oxidative glutamate toxicity. J. Neurosci. 16:6394–6401; 1996.
[14] Froissard, P.; Monrocq, H.; Duval, D. Role of glutathione metabolism in the glutamate-induced programmed cell death of neuronal-like PC12 cells. Eur. J. Pharmacol. 326:93–99; 1997.
[15] Ratan, R. R.; Murphy, T. H.; Baraban, J. M. Oxidative stress induces apoptosis in embryonic cortical neurons. J. Neurochem. 62:376–379; 1994.
[16] Oka, A.; Belliveau, M. J.; Rosenberg, P. A.; Volpe, J. J. Vulnerability of oligodendroglia to glutamate: pharmacology, mechanisms, and prevention. J. Neurosci. 13:1441–1453; 1993.

[17] Chen, C. J.; Liao, S. L.; Kuo, J. S. Gliotoxic action of glutamate on cultured astrocytes. *J. Neurochem.* **75:**1557–1565; 2000.

[18] Tan, S.; Wood, M.; Maher, P. Oxidative stress induces a form of programmed cell death with characteristics of both apoptosis and necrosis in neuronal cells. *J. Neurochem.* **71:**95–105; 1998.

[19] Li, Y.; Maher, P.; Schubert, D. A role for 12-lipoxygenase in nerve cell death caused by glutathione depletion. *Neuron* **19:**453–463; 1997.

[20] Tan, S.; Sagara, Y.; Liu, Y.; Maher, P.; Schubert, D. The regulation of reactive oxygen species production during programmed cell death. *J. Cell Biol.* **141:**1423–1432; 1998.

[21] Li, Y.; Maher, P.; Schubert, D. Requirement for cGMP in nerve cell death caused by glutathione depletion. *J. Cell Biol.* **139:**1317–1324; 1997.

[22] Lewerenz, J.; Klein, M.; Methner, A. Cooperative action of glutamate transporters and cystine/glutamate antiporter system Xc- protects from oxidative glutamate toxicity. *J. Neurochem.* **98:**916–925; 2006.

[23] Dittmer, S.; Sahin, M.; Pantlen, A.; Saxena, A.; Toutzaris, D.; Pina, A. L.; Geerts, A.; Golz, S.; Methner, A. The constitutively active orphan G-protein-coupled receptor GPR39 protects from cell death by increasing secretion of pigment epithelium-derived growth factor. *J. Biol. Chem.* **283:**7074–7081; 2008.

[24] Sahin, M.; Joost, P.; Saxena, A.; Lewerenz, J.; Methner, A. Induction of Bcl-2 by functional regulation of G-protein coupled receptors protects from oxidative glutamate toxicity by increasing glutathione. *Free Radic. Res.* **40:**1113–1123; 2006.

[25] Sturtz, L. A.; Diekert, K.; Jensen, L. T.; Lill, R.; Culotta, V. C. A fraction of yeast Cu,Zn-superoxide dismutase and its metallochaperone, CCS, localize to the intermembrane space of mitochondria. *J. Biol. Chem.* **276:**38084–38089; 2001.

[26] Liu, X. F.; Elashvili, I.; Gralla, E. B.; Valentine, J. S.; Lapinskas, P.; Culotta, V. C. Yeast lacking superoxide dismutase: isolation of genetic suppressors. *J. Biol. Chem.* **267:**18298–18302; 1992.

[27] Slekar, K. H.; Kosman, D.; Culotta, V. C. The yeast copper/zinc superoxide dismutase and the pentose phosphate pathway play overlapping roles in oxidative stress protection. *J. Biol. Chem.* **271:**28831–28836; 1996.

[28] Gietz, R. D.; Schiestl, R. H. Applications of high efficiency lithium acetate transformation of intact yeast cells using single-stranded nucleic acids as carrier. **7:**253–263; 1991.

[29] Gralla, E. B.; Kosman, D. J. Molecular genetics of superoxide dismutases in yeasts and related fungi. *Adv. Genet.* **30:**251–319; 1992.

[30] Townsend, A. J.; Leone-Kabler, S.; Haynes, R. L.; Wu, Y.; Szweda, L.; Bunting, K. D. Selective protection by stably transfected human ALDH3A1 (but not human ALDH1A1) against toxicity of aliphatic aldehydes in V79 cells. *Chem. Biol. Interact.* **130-132:**261–273; 2001.

[31] Neuberger, G.; Maurer-Stroh, S.; Eisenhaber, B.; Hartig, A.; Eisenhaber, F. Prediction of peroxisomal targeting signal 1 containing proteins from amino acid sequence. *J. Mol. Biol.* **328:**581–592; 2003.

[32] Bannister, J. V.; Bannister, W. H.; Rotilio, G. Aspects of the structure, function, and applications of superoxide dismutase. *CRC Crit. Rev. Biochem.* **22:**111–180; 1987.

[33] Culotta, V. C.; Klomp, L.; Strain, J.; Casareno, R.; Krems, B.; Gitlin, J. D. The copper chaperone for superoxide dismutase. *J. Biol. Chem.* **272:**23469–23472; 1997.

[34] Sagara, Y.; Dargusch, R.; Chambers, D.; Davis, J.; Schubert, D.; Maher, P. Cellular mechanisms of resistance to chronic oxidative stress. *Free Radic. Biol. Med.* **24:**1375–1389; 1998.

[35] Sagara, Y.; Ishige, K.; Tsai, C.; Maher, P. Tyrphostins protect neuronal cells from oxidative stress. *J. Biol. Chem.* **277:**36204–36215; 2002.

[36] Tan, S.; Somia, N.; Maher, P.; Schubert, D. Regulation of antioxidant metabolism by translation initiation factor 2alpha. *J. Cell Biol.* **152:**997–1006; 2001.

[37] Lindahl, R. Aldehyde dehydrogenases and their role in carcinogenesis. *Crit. Rev. Biochem. Mol. Biol.* **27:**283–335; 1992.

[38] Nebert, D. W. Drug-metabolizing enzymes, polymorphisms and interindividual response to environmental toxicants. *Clin. Chem. Lab. Med.* **38:**857–861; 2000.

[39] Zimatkin, S. M. Histochemical study of aldehyde dehydrogenase in the rat CNS. *J. Neurochem.* **56:**1–11; 1991.

[40] Iourgenko, V.; Zhang, W.; Mickanin, C.; Daly, I.; Jiang, C.; Hexham, J. M.; Orth, A. P.; Miraglia, L.; Meltzer, J.; Garza, D.; Chirn, G. W.; McWhinnie, E.; Cohen, D.; Skelton, J.; Terry, R.; Yu, Y.; Bodian, D.; Buxton, F. P.; Zhu, J.; Song, C.; Labow, M. A. Identification of a family of cAMP response element-binding protein coactivators by genome-scale functional analysis in mammalian cells. *Proc. Natl. Acad. Sci. USA* **100:**12147–12152; 2003.

[41] Santos, M. J.; Quintanilla, R. A.; Toro, A.; Grandy, R.; Dinamarca, M. C.; Godoy, J. A.; Inestrosa, N. C. Peroxisomal proliferation protects from beta-amyloid neurodegeneration. *J. Biol. Chem.* **280:**41057–41068; 2005.